DOI: 10.24996/ijs.2022.63.7.35

ISSN: 0067-2904

Mathematical Analysis of Peristaltic Pumps for Fene-P model subject to Hall and Joule impact

Saba S. Hasen[1]*, Rabiha S. Kareem[2], Hayat A.Ali[3]

[1]*Department of Applied Science, University of Technology, Baghdad, Iraq*
[2]*University of Information Technology and Communications, Baghdad, Iraq*
[3]*Department of Applied Science, University of Technology, Baghdad, Iraq*

Received: 6/10/2020 Accepted: 13/1/2022 Published: 30/7/2022

Abstract

A mathematical model is developed to discuss the impact of the Hall current and the Joule heating on the peristaltic flux of finitely extensible nonlinear elastic Peterlin (FENE-P) fluid in a tapered tube with mild stenosis. The fluid movement along the wall surface resulted from the sinusoidal wave flowing with constant speed. Conditions of velocity and thermal slip are applied. Lubrication approximation is adopted to modify the governing flow problem. To discover the solution to a system of equations, the regular perturbation approach is used. The effects of the different physical parameters are debated and graphically shown in a set of figures. It is discovered that as the Hall current parameter is increased and the Hartman number is decreased, the fluid velocity increases. It is also worth noting that the Dufour number causes the fluid temperature to rise, whilst the Hall current parameter causes the temperature to fall. In the meantime, both the Hall current parameter and the Soret number have the opposite effect on concentration. The trapping phenomenon is thoroughly investigated.

Keywords: FENE-P fluid, Hall effects, Joule heating, Peristalsis, Slip conditions.

التحليل الرياضي للضخ التمعجي لنموذج فاين- بي الخاضع لتأثير هول وجول

صبا ستار حسن[1]*, رابحة سليم كريم[2], حياة عادل علي[3]

[1]قسم العلوم التطبيقية, الجامعة التكنولوجية, بغداد,العراق
[2]جامعة تكنولوجية المعلومات والاتصالات, بغداد, العراق
[3]قسم العلوم التطبيقية, الجامعة التكنولوجية, بغداد,العراق

الخلاصة

تم تطوير نموذج رياضي لمناقشة تأثير تيار هول وتسخين جول على التدفق التمعجي لسائل بيترلين المرن غير الخطي (FENE-P) في أنبوب مدبب مع تضيق خفيف. نتجت حركة السوائل على طول سطح الجدار عن تدفق الموجة الجيبية بسرعة ثابتة. يتم تطبيق شروط السرعة والانزلاق الحراري. تم اعتماد تقريب التزييت لتبسيط مشكلة التدفق الحاكمة. لاكتشاف الحل لنظام المعادلات ، يتم استخدام نهج الاضطراب المنتظم. تمت مناقشة تأثيرات المعلمات الفيزيائية المختلفة وعرضها بيانياً عن طريق مجموعة من الأشكال. تم

*Email: saba.s.hasen@uotechnology.edu.iq

اكتشاف أنه مع زيادة معلمة تيار هول وانخفاض رقم هارتمان ، تزداد سرعة السائل. وتجدر الإشارة أيضًا إلى أن رقم دوفور يتسبب في ارتفاع درجة حرارة السائل ، في حين يتسبب معلمة تيارهول في انخفاض درجة الحرارة. في غضون ذلك ، يكون لكل من معلمة تيار هول ورقم سورت تأثير معاكس على التركيز. يتم التحقيق بدقة في ظاهرة االبلعة.

1. Introduction

Peristalsis is a vital system for transferring fluids through a tube by using a contractile ring above the tube to propel the material ahead. This mechanism is critical for the movement of fluids in living beings and industries. The peristaltic phenomenon is what makes dialysis and heart-lung machines work. The authors in [1–8] show recent attempts at peristaltic flow effects.

The majority of fluids in nature have non-Newtonian properties. Under the stress, non-Newtonian fluids change their viscosity or flow behavior, when the stress is applied we note that not every non-newtonian fluids have the same response, some grow more solid, whereas others become more fluid. Some non-Newtonian fluids interact in response to the magnitude of the stress applied, whereas others react in response to the duration of the stress. The FENE-P model is a non-Newtonian model that has been widely used to correlate experimental data on shear and extensional viscosities, as well as transient and normal stress variations in polymer solutions. Paper pulps are the polymer solutions, while chyme, a biological fluid, is characterized as a pulpy acidic fluid. The FENE-P model is widely used rheological constitutive equation for polymeric liquids. Because chyme and pulps are similar, they can be used to represent the rheological properties of chyme while researching the peristaltic transpose of chyme. Furthermore, it is capable of simulating viscometric characteristics for a wide range of fluids and can forecast decreasing viscosity with shear. Ali et al.[9] studied the peristaltic motion of two fluids, namely the FENE-P and the Newtonian fluids in a flexible tube under the effect of electro-osmotic force. Asghar et al.[10] presented the heat and mass transfer impact on peristaltic flow of (FENE-P) fluid in the presence of chemical reaction. Refs.[11-14] contains several important assessments on the usage of the FENE-P fluid model in mathematical modeling and investigation of various flow circumstances.

The examination of Hall's influence becomes extremely important in the presence of a high magnetic field. These effects are most useful in a variety of industries, including power generators, magnetometers for measuring magnetic fields, transformers, the sensors of Hall current, car fuel level indicators, spacecraft propulsion, and magnetic situation monitoring in DC electric motors. Hayat et al. [15] investigated the Hall current influence on the peristaltic motion of Eyring–Powell fluid in an inclined symmetric tube. EL-Dabe et al. [16] studied the influence of the Hall current and Joule heating on the peristaltic transfer of a Sisko fluid through a porous medium. the Hall current effects are reported in Refs. [17-19]).

Heat transfer has an important role in peristaltic movements, n particular, the blood flows. Some of the most common uses of heat transfer are conduction of heat in tissues, radiative heat transfer between surface and environment, heat transfer by convection when the blood flux from pores of tissue, vasodilation and food preparation. Heat transfer is involved in peristalsis processes such as oxygenation and hemodialysis.In addition, it has several implementations in engineering encompassing high temperatures through variable thermal conductivity. Such operations include turbines, space vehicles, nuclear power plants, pumps operated at high temperatures and rockets. As the electric energy is transformed into heat, Joule heating happens. Soldering irons, electric stoves, electric heaters and cartridge heaters are all examples of Joule heating. Furthermore, electronic cigarettes mainly operate on the Joule heating principle. Many investigators and studies have presented discussions in [20-26]

The goal of this study is to look at how the Hall current, Joule heating, peristalsis and the Soret and Dufour impact affect a fully developed convection flow in a tapered tube with slight stenosis. Using the long wavelength and low Reynolds number presumptions, the governing equations of motion have been simplified. These equations are approximately resolved under the required boundary conditions by employing a perturbation method, see[27].

2. Problem formulation

Consider that an incompressible viscoelastic fluid bearing the peristaltic flow in a tapered tube. The motion of the fluid is created by sinusoidal wave train conduction along the walls of the tube with mild stenosis. The magnetic field of uniform strength $B_0$is acting upon the fluid, however, the influence of the electric field is not applied. While it is taken into account the effect of the Hall and Joule heating. We consider a cylindrical polar coordinate $(\bar{R},\bar{\theta},\bar{Z})$ in such a way that the Z-axis synchronizes with the axis of the tubes. Hall's current presence creates a force in the θ-direction. As the result, the flow of fluid becomes three dimensions, however, there is no influence on the fluid flow, concentration properties and heat transfer in θ direction. The tube is convectively heated. Also, the condition of convective mass is applied in the physical Sketch of the situation of the problem that is illustrated in Figure -1.

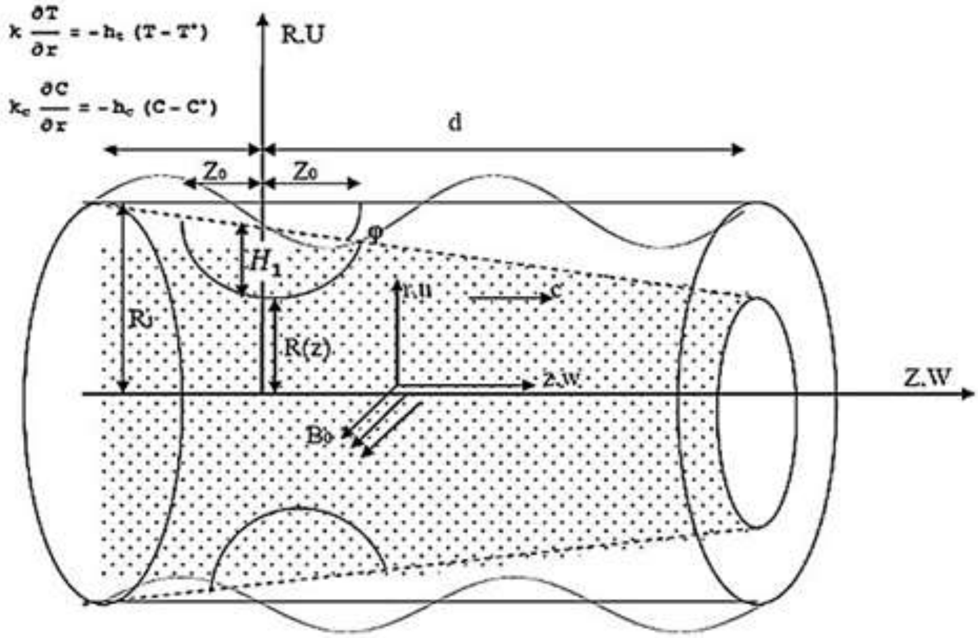

Figure 1-The geometry of the problem

Travelling waves of small amplitudes propagating along tapered walls of the tube are taken as follows:

$$R_2(\bar{Z},t) = R(\bar{Z}) + \bar{H}_1$$
$$R(Z) = \begin{cases} R_1 - \delta\, m_1(\bar{Z}+\bar{L}+\bar{d}) & -\bar{L} \le \bar{Z} < -\bar{Z}_0 \\ R_1 - \delta\, m_1(\bar{Z}+\bar{L}+\bar{d}) - \frac{H_0}{2}(1+\cos\frac{\pi\bar{Z}}{Z_0}) & -\bar{Z}_0 \le \bar{Z} \le \bar{Z}_0 \\ R_1 - \delta\, m_1(Z+\bar{L}+\bar{d}) & \bar{Z}_0 < \bar{Z} \le \bar{d} \end{cases} \tag{1}$$

$\bar{H}_1 = \bar{\epsilon}\cos\frac{2\pi}{\lambda}(\bar{Z}-ct)$, $\bar{H}_0 = \bar{h}\cos\varphi$.

where $R(Z)$ indicates the efficient radius of the tapered tube, $\overline{H_1}$ represents the peristaltic wall geometry, the radius of the tube is denoted by R_1, $\overline{Z_0}$ is the half-length of the stenosis, δ is the wavelength, λ is the wavelength, $\bar{\epsilon}$ is wave amplitude, $c = \frac{k}{R_1}$ is the wave velocity, φ is the angle of tapering, t is the time, $m_1 = \tan\varphi$ is the slope of the tapered tube, $\overline{H}_0$ is the height of the stenosis in a tapered tube and $\bar{h}$ is the maximum height of the stenosis.

In our study, the walls of the tube are supposed to be electrically insulated. When the electrically conducting fluid influxes through the tube in the existence of a magnetohydrodynamic field, the generalized Ohm's law with the Hall effect can be expressed as

$$J = \sigma[E + \bar{V} \times B - \frac{1}{en}(J \times B)] \tag{2}$$

where e is the electric charge of ions, n is the number density of electrons, and $E = 0$. the magnetic field represent as $B = (0, \beta_0, 0)$, while the influx velocity of the fluid is given as follows $\bar{V} = (\bar{U}, 0, \bar{W})$, hence we have

$$J \times B = -\frac{\sigma\beta_0^2}{1+m^2}[(\bar{U} + m\bar{W}), 0, (\bar{W} - m\bar{U})] \tag{3}$$

where $m = \frac{\sigma\beta_0}{e\,n}$ is the Hall current parameter.

The four nonlinear partial differential equations that are connected (continuity, momentum, energy, and mass diffusion) describe the fluid flow in the frame $(\bar{R}, \bar{Z})$ are expressed by

$$\frac{\partial\bar{U}}{\partial\bar{R}} + \frac{\bar{U}}{\bar{R}} + \frac{\partial\bar{W}}{\partial\bar{Z}} = 0, \tag{4}$$

$$\rho\left(\frac{\partial\bar{U}}{\partial\bar{t}} + \bar{U}\frac{\partial\bar{U}}{\partial\bar{R}} + \bar{W}\frac{\partial\bar{U}}{\partial\bar{Z}}\right) = -\frac{\partial\bar{P}}{\partial\bar{R}} + \frac{1}{\bar{R}}\frac{\partial}{\partial\bar{R}}(\bar{R}\bar{S}_{\bar{R}\,\bar{R}}) + \frac{\partial}{\partial\bar{Z}}(\bar{S}_{\bar{R}\,\bar{Z}}) - \frac{\bar{S}_{\bar{\theta}\,\bar{\theta}}}{\bar{R}} - \frac{\sigma\beta_0^2}{1+m^2}(\bar{U} + m\bar{W} \tag{5}$$

$$\rho\left(\frac{\partial\bar{W}}{\partial\bar{t}} + \bar{U}\frac{\partial\bar{W}}{\partial\bar{R}} + \bar{W}\frac{\partial\bar{W}}{\partial\bar{Z}}\right) = -\frac{\partial\bar{P}}{\partial\bar{Z}} + \frac{1}{\bar{R}}\frac{\partial}{\partial\bar{R}}(\bar{R}\bar{S}_{\bar{R}\,\bar{Z}}) + \frac{\partial}{\partial\bar{Z}}(\bar{S}_{\bar{Z}\,Z}) - \frac{\sigma\beta_0^2}{1+m^2}(\bar{W} - m\bar{U}), \tag{6}$$

$$\rho c_p\left(\frac{\partial\bar{T}}{\partial\bar{t}} + \bar{U}\frac{\partial\bar{T}}{\partial\bar{R}} + \bar{W}\frac{\partial\bar{T}}{\partial\bar{Z}}\right) = \kappa\left(\frac{\partial^2\bar{T}}{\partial\bar{R}^2} + \frac{1}{\bar{R}}\frac{\partial\bar{T}}{\partial\bar{R}} + \frac{\partial^2\bar{T}}{\partial\bar{Z}^2}\right) + \frac{D_m K_T}{C_s}\left(\frac{\partial^2\bar{C}}{\partial\bar{R}^2} + \frac{1}{\bar{R}}\frac{\partial\bar{C}}{\partial\bar{R}} + \frac{\partial^2\bar{C}}{\partial\bar{Z}^2}\right) + \frac{\sigma\beta_0^2}{1+m^2}(\bar{W}^2 + \bar{U}^2), \tag{7}$$

$$\left(\frac{\partial\bar{C}}{\partial\bar{t}} + \bar{U}\frac{\partial\bar{C}}{\partial\bar{R}} + \bar{W}\frac{\partial\bar{C}}{\partial\bar{Z}}\right) = D_m\left(\frac{\partial^2\bar{C}}{\partial\bar{R}^2} + \frac{1}{\bar{R}}\frac{\partial\bar{C}}{\partial\bar{R}} + \frac{\partial^2\bar{C}}{\partial\bar{Z}^2}\right) + \frac{D_m K_T}{T_m}\left(\frac{\partial^2\bar{T}}{\partial\bar{R}^2} + \frac{1}{\bar{R}}\frac{\partial\bar{T}}{\partial\bar{R}} + \frac{\partial^2\bar{T}}{\partial\bar{Z}^2}\right). \tag{8}$$

where $\bar{U}, \bar{W}$ are the velocity components in $\bar{R}$ and $\bar{Z}$ directions, respectively and $\bar{S}_{ij}$ $\bar{P}, \bar{T}, \bar{C}$, K_T, D_m $, T_m, \rho, c_p$ are $\bar{S}_{ij}$ assigns the extra stress tensor over a phase whose normal is the i-direction and act on the face j- direction, pressure, fluid temperature, the concentration of fluid, thermal diffusion, coefficient of thermal diffusivity, the mean fluid temperature, the fluid density and the specific heat, respectively.

The partial slip condition together with the convective boundary conditions of the wall can be expressed as follows:

$$\left.\begin{array}{c} \bar{U} = 0, \frac{\partial\bar{W}}{\partial\bar{R}} = 0, \frac{\partial\bar{T}}{\partial\bar{R}} = 0, \frac{\partial\bar{C}}{\partial\bar{R}} = 0 \;\; at\; \bar{R} = 0 \\ \bar{U} = \frac{\partial H_1}{\partial t},\; \bar{W} = -\gamma S_{RZ},\; K\frac{\partial\bar{T}}{\partial\bar{R}} = -h_t(\bar{T} - \bar{T}_0),\; D_m\frac{\partial\bar{C}}{\partial\bar{R}} = -h_c(\bar{C} - \bar{C}_0)\; at\; \bar{R}_2 \end{array}\right\} \tag{9}$$

where γ is the slip parameter, h_t stands for heat transfer coefficient, and it reflects the proportionality constant between the heat flux and the thermodynamic driving force for the flow of the heat. Meanwhile, the mass transfer coefficient, abbreviated as h_c, is used to represent the relationship between the flux of actual mass of kinds into or out of moving fluid and the driving force for that flow.

The constitutional equations for a FENE-P fluid model are defined as

$$f\,(tr(\bar{S})\bar{S} + \lambda_p\overset{\nabla}{\bar{S}} = 2b\mu D, \tag{10}$$

$$\overset{\nabla}{\bar{S}} = \frac{\partial\bar{S}}{\partial t} + (\bar{V}\cdot\nabla)\bar{S} - \bar{S}(\nabla\bar{V})^T - (\nabla\bar{V})\bar{S}. \tag{11}$$

And the functions $f\,(tr(\bar{S})$ and D are given by

$$f\,(tr(\bar{S})) = 1 + \frac{3b + \frac{\lambda_p}{\mu}(tr(\bar{S}))}{L^2}, D = \frac{1}{2}(\nabla\bar{V} + (\nabla\bar{V})^T) \tag{12}$$

where $tr(\bar{S}) = \bar{S}_{\bar{R}\,\bar{R}} + \bar{S}_{\bar{\theta}\,\bar{\theta}} + \bar{S}_{\bar{Z}\,Z}$, and the parameter $b = 1/(1 - 3/\bar{L}^2)$ is dependent on $\bar{L}^2$ which is represented the extensibility parameter, λ_p is the relaxation time, μ is the zero shear rate polymer viscosity.

The Galilean transformations are utilized to transform laboratory frame into periodic ones to facilitate the governing Eqs. (4)–(8), which are given as

$$\bar{r} = \bar{R},\ \bar{z} = \bar{Z} - ct,\ \bar{w} = \bar{W} - c,\ \bar{u} = \bar{U} \tag{13}$$

Now, we are introducing non-dimensional scaling transformations as follows:

$$\left.\begin{array}{l} r = \frac{\bar{r}}{R_1},\ z = \frac{\bar{z}}{\lambda},\ u = \frac{\bar{u}}{\delta c}, w = \frac{\bar{w}}{c},\ H_1 = \frac{\bar{H}_1}{R_1}, \delta = \frac{R_1}{\lambda}, S = \frac{R_1 \bar{S}}{c\mu}, z_0 = \frac{\bar{z}_0}{\lambda}, \epsilon = \frac{\bar{\epsilon}}{R_1} \\ L = \frac{\bar{L}}{\lambda},\ h = \frac{\bar{h}}{R_1}, d = \frac{\bar{d}}{\lambda}, R(z) = \frac{\bar{R}(z)}{R_1}, P = \frac{R_1^2 P}{c\lambda\mu}, T = \frac{\bar{T} - T_0}{\beta R_1}, C = \frac{\bar{C} - C_0}{C_0}, \gamma^* = \frac{\mu}{R_1}\gamma \\ H = \sqrt{\frac{\sigma}{\mu}}\beta_0 R_1, Q = \frac{\bar{Q}}{2\pi R_1^2 c}, R_e = \frac{cR_1\rho}{\mu}, B_r = P_r E_c, D_e = \frac{\lambda_p c}{R_1}, E_c = \frac{c^2}{c_p \beta R_1}, \\ \beta_t = \frac{h_t R_1}{K}, \beta_c = \frac{h_c R_1}{D_m} S_c = \frac{\mu}{\rho D_m}, P_r = \frac{\mu c_p}{\kappa},\ D_u = \frac{D_m K_T C_0}{\mu C_s \beta R_1 c_p}, S_r = \frac{\rho D_m K_T \beta R_1}{\mu T_m C_0} \end{array}\right\} \tag{14}$$

where H is the Hartman number, Q is volumetric flow rate, R_e is Reynold's number, β_t is the heat transfer Biot number, β_c is the mass transfer Biot number, B_r is the Brickman number, D_e is the Deborah number, S_c is the Schmidt number, P_r is the Prandtl number, D_u is the Dufour number, S_r is the Soret number, and β is the adverse temperature gradient.

Now by employment the above transformations Eqs. (13)-(14) into the nonlinear system (4-8), we get the following formulas

$$\frac{\partial u}{\partial r} + \frac{u}{r} + \frac{\partial w}{\partial z} = 0, \tag{15}$$

$$Re\,\delta^3 \left(u\frac{\partial u}{\partial r} + (w+1)\frac{\partial u}{\partial z} \right) = -\frac{\partial p}{\partial r} + \delta \frac{1}{r}\frac{\partial}{\partial r}(r\,S_{rr}) + \delta^2 \frac{\partial}{\partial z} S_{rz} - \delta \frac{S_{\theta\theta}}{r} - \frac{H^2}{1+m^2}\delta^2 u - \frac{H^2}{1+m^2}\delta\, m(w+1), \tag{16}$$

$$Re\delta \left(u\frac{\partial w}{\partial r} + (w+1)\frac{\partial w}{\partial z} \right) = -\frac{\partial p}{\partial z} + \frac{1}{r}\frac{\partial}{\partial r}(rS_{rz}) + \delta \frac{\partial}{\partial \bar{z}}(S_{zz}) - \frac{H^2}{1+m^2}(w+1) + \frac{H^2}{1+m^2}\delta\, u, \tag{17}$$

$$Re\, P_r \delta \left(u\frac{\partial T}{\partial r} + (w+1)\frac{\partial T}{\partial z} \right) = \frac{\partial^2 T}{\partial r^2} + \frac{1}{r}\frac{\partial T}{\partial r} + \delta^2 \frac{\partial^2 T}{\partial z^2} + D_u P_r \left(\frac{\partial^2 C}{\partial r^2} + \frac{1}{r}\frac{\partial C}{\partial r} \right) + \frac{H^2}{1+m^2} B_r((w+1)^2 + \delta^2 u^2), \tag{18}$$

$$R_e S_c \delta \left(u\frac{\partial C}{\partial r} + (w+1)\frac{\partial C}{\partial z} \right) = \frac{\partial^2 C}{\partial r^2} + \frac{1}{r}\frac{\partial C}{\partial r} + \delta^2 \frac{\partial^2 C}{\partial z^2} + S_r S_c \left(\frac{\partial^2 T}{\partial r^2} + \frac{1}{r}\frac{\partial T}{\partial r} \right) + S_r S_c \delta^2 \frac{\partial^2 T}{\partial z^2}, \tag{19}$$

And by reusing the previous transformations on Eq. (10), we get

$$fS_{rr} + \delta\, D_e \left(u\frac{\partial S_{rr}}{\partial r} + (w+1)\frac{\partial S_{rr}}{\partial z} \right) - \delta\, D_e \left(2S_{rr}\frac{\partial u}{\partial r} - 2S_{rz}\frac{\partial u}{\partial z} \right) = 2b\delta \frac{\partial u}{\partial r}, \tag{20}$$

$$fS_{rz} + \delta\, D_e \left(u\frac{\partial S_{rz}}{\partial r} + (w+1)\frac{\partial S_{rz}}{\partial z} \right) - \left(\delta\, D_e S_{rz}\frac{\partial u}{\partial r} + \delta^2\, D_e S_{zz}\frac{\partial u}{\partial z} \right) - D_e S_{rr}\frac{\partial w}{\partial r} - \delta\, D_e S_{rz}\frac{\partial w}{\partial z} = b\delta^2 \frac{\partial u}{\partial z} + b\frac{\partial w}{\partial r}, \tag{21}$$

$$fS_{zz} + \delta\, D_e \left(u\frac{\partial S_{zz}}{\partial r} + (w+1)\frac{\partial S_{rz}}{\partial z} \right) - 2\, D_e S_{rz}\frac{\partial w}{\partial r} - 2\delta\, D_e S_{zz}\frac{\partial w}{\partial z} = 2b\delta \frac{\partial w}{\partial z}. \tag{22}$$

We note that Eqs. (15) - (22) are difficult to deal with, so through our observation of the literature, there is no attempt to address the peristaltic fluid problem of non-Newtonian fluids without applying some assumptions. Fortunately, because of the association of peristaltic movement with physiology, suitable assumptions can be used, for example, in the movement of the intestines where the fluid motion is peristaltic, the vessel radius is so small compared to the wavelength of the wave.

The above two assumptions are commonly referred to low Reynolds number and long wavelength and assumptions in the literature. The parameter characterizing the ratio of the channel radius to the wavelength of the peristaltic wave in our study is δ. Thus, for the flow under consideration, we assume $\delta \approx 0$ and $R_e \approx 0$. Under the above assumptions, Eqs. (16)-(22) have the following formula

$$\frac{\partial p}{\partial r}=0, \tag{23}$$

$$-\frac{\partial p}{\partial z}+\frac{1}{r}\frac{\partial}{\partial r}(rS_{rz})+\frac{H^2}{1+m^2}(w+1)=0, \tag{24}$$

$$\frac{\partial^2 T}{\partial r^2}+\frac{1}{r}\frac{\partial T}{\partial r}+\ D_uP_r\left(\frac{\partial^2 C}{\partial r^2}+\frac{1}{r}\frac{\partial C}{\partial r}\right)+\frac{H^2}{1+m^2}B_r((w+1)^2=0, \tag{25}$$

$$\frac{\partial^2 C}{\partial r^2}+\frac{1}{r}\frac{\partial C}{\partial r}+S_rS_c\left(\frac{\partial^2 T}{\partial r^2}+\frac{1}{r}\frac{\partial T}{\partial r}\right)=0, \tag{26}$$

And

$$fS_{rr}=0, \tag{27}$$

$$fS_{rz}-\ D_eS_{rr}\frac{\partial w}{\partial r}=b\frac{\partial w}{\partial r}, \tag{28}$$

$$fS_{zz}-2\ D_eS_{rz}\frac{\partial w}{\partial r}=0, \tag{29}$$

With the final formula of the dimensionless boundary conditions

$$\left.\begin{array}{l} u=0,\frac{\partial w}{\partial r}=0,\frac{\partial T}{\partial r}=0,\frac{\partial C}{\partial r}=0 \quad at \quad r=0 \\ u=\frac{\partial H_1}{\partial t}=2\pi\epsilon\sin 2\pi z\,,w=-1-\gamma^* S_{rz},\frac{\partial T}{\partial r}=-\beta_t T,\frac{\partial C}{\partial r}=-\beta_c C \quad at \quad r_2 \end{array}\right\}, \tag{30}$$

And we can define the stream $\psi(r,z,t)$ function as follows

$$w=\frac{1}{r}\frac{\partial\psi}{\partial r},u=-\frac{1}{r}\frac{\partial\psi}{\partial z}. \tag{31}$$

3. Solution Methodology

In this section, we refuge to use the approximate method to get the solution of the system. The regular perturbation technique is employed to find accurate approximate to Eqs. (23)-(29).

Frist simplifying and solving the system (27)-(29) yield the normal components of the extra stress tensor

$$S_{zz}=\frac{2D_e}{b}S_{rz}^2,\ \text{and}S_{rr}=S_{\theta\theta}=S_{r\theta}=S_{\theta z}=0 \tag{32}$$

So the system can be reduced to

$$\left(b+\frac{2D_e^2}{bL^2}S_{rz}^2\right)S_{rz}=b\frac{\partial w}{\partial r} \tag{33}$$

The used technique depends on choosing a small parameter, in our study, we choose a parameter H to solve the nonlinear system. The following expansions are used to obtain the perturbed solution

$$\left.\begin{array}{l} \psi=\psi_0+H^2\,\psi_1+O(H^4) \\ S_{rz}=S_{rz_0}+H^2\,S_{rz_1}+O(H^4) \\ T=T_0+H^2\,T_1+O(H^4) \\ C=C_0+H^2\,C_1+O(H^4) \\ p=p_0+H^2p_1\ +O(H^4) \end{array}\right\} \tag{34}$$

Now we will employ these physical quantities into Eqs. (23)- (26) and boundary conditions (30), and then gathering the like powers of H^2, we obtain the corresponding zero- and first-order systems. By solving the system, we get the solution as below:

$$\psi_0=\frac{r^2(-48b^2L^2-6b^2L^2(2r_2{}^2-r^2+4r_2\gamma)p_0+\mathrm{D}_e{}^2(-3r_2{}^4+r^4)p_0{}^3}{96b^2L^2}, \tag{35}$$

$$\psi_1=\frac{1}{46080b^4L^4(1+m^2)}r^2(120b^4L^4(9r_2{}^4+r^4+36r_2{}^3\gamma-12hr_2{}^2\gamma-6r_2{}^2(r^2-8\gamma^2))p_0+20b^2\mathrm{D}_e{}^2L^2(52r_2{}^6-9r_2{}^4r^2-18r_2{}^2r^4+5r^6+132r_2{}^5\gamma-36r_2r^4\gamma)p_0^3+9\mathrm{D}_e{}^4(-5r_2{}^4+r^4)^2p_0^5-2880b^4L^4(1+m^2)(2r_2{}^2-r^2+4r_2\gamma)p_1-1440b^2\mathrm{D}_e{}^2L^2(1+m^2)(3r_2{}^4-r^4)p_0^2p_1), \tag{36}$$

$$T_0=0, \tag{37}$$

$T_1 = -\frac{1}{460800b^4L^4(1+m^2)\beta_t(-1+D_uP_rS_rS_c)} B_r p_0^2(400b^4L^4(11{r_2}^6\beta_t - 2r^6\beta_t + 18hr^4\beta_t\gamma - 72{r_2}^3(r^2\beta_t - 2\gamma)\gamma + 6{r_2}^5(2+9\beta_t\gamma) + 9{r_2}^2r^2\beta_t(r^2 - 8\gamma^2) - \cdots,$
(38)

$$C_0 = 0, \quad (39)$$

$C_1 = \frac{1}{460800b^4L^4(1+m^2)\kappa(-1+D_uP_rS_rS_c)}(4800b^4B_r{r_2}^5L^4p_0^2S_rS_c + 28800b^4B_r{r_2}^4L^4\gamma p_0^2S_rS_c + 57600b^4B_r{r_2}^3L^4\gamma^2p_0^2S_rS_c + \cdots,$ (40)

Based on the above equations, the velocity of the fluid is:

$w = \frac{1}{4608b^4L^4(1+m^2)}(72b^4L^4(3h^4H^2 + r^2(16+16m^2+H^2r^2) + 12h^3H^2\gamma - 8h(4 + 4m^2 + H^2r^2)\gamma - 4h^2(4+4m^2+H^2(r^2-4\gamma^2)))p_0 + \cdots.$ (41)

4. Results and discussion

The solution of a non-Newtonian viscoelastic fluid with a tapered tube is dealt with in this section. The expression for the velocity, temperature, concentration and stream function is computed approximately for various flow parameters. Mathematica program (version 11.0) has been employed to calculate the influence of embedded parameters on the hydrodynamic and thermal behavior which are represented by the Hartman number H, the Hall current m, the Deborah number D_e, the slip parameter γ, the Brickman number B_r, the Dufour number D_u, the Soret number S_r, the mass transfer Biot number β_c. Figures 2 and 3 show the magnetic field and the Hall effect on the velocity profile for values of H and m. It is depicted that the velocity with the increase in the magnetic field, velocity profile decreases at tube sides while Figure- 3 depicts that the Hall current enhances the flow of fluid. Figure- 4 illustrates the velocity variation vs r-axis for various values of D_e. It is clear that the velocity of the fluid is reduced when D_e increases. Figure-5 indicates that the velocity profile decreases for the larger value of momentum slip parameter γ. Figure- 6 shows the evolution in temperature for different values of H.it is exhibited that for large values of H the temperature distribution increases at the center of the tube whereas it is the opposite at the sides. Figure- 7 indicates that by increasing m the temperature increases at the edges of the channel while decreasing at the center. The difference of temperature for various values of B_r, is demonstrated in Figure-8. It is observed that The temperature rises with B_r. This position can be interpreted as the thermal energy generated as a result of the dissipation of the viscous. So, the temperature of fluid increases. In Figure-9, the impact of D_u on temperature is clarified. It can be observed that the heat enhances with the boost of D_u value. In Figures- 10-13 the profiles of concentration are shown for different values of the parameters of interest where it is found in Figure- 10 that the concentration of fluid rises with H near the wall but decreases at the center of the tube. Figure- 11 shows that concentration gets increasing function in $(-1.5 \leq r \leq 1.5)$ while it gets the opposite attitude at the walls. Figure-12 shows that an increase in S_r leads to a decrease in the concentration of fluid. Figure-13 indicates that the mass diffusion increases for the larger value of β_c. The formation of a bolus by internally splitting streamlines is called trapping. The bolus proceeds forward through a peristaltic wave with the same speed. Figure-14 depicts the streamlines for the various magnitude of H, it is clear that by increasing the value of H the number of the trapped bolus is increasing while the size of trapping decreases. Figure-15 illustrates that by increasing the value of D_e, the number of the trapped bolus is decreasing whereas the size increases. The impact of the slip parameter γ on the trapping is displayed in Figure- 16. The bolus increases in number while the decrease in size by the increase of γ.

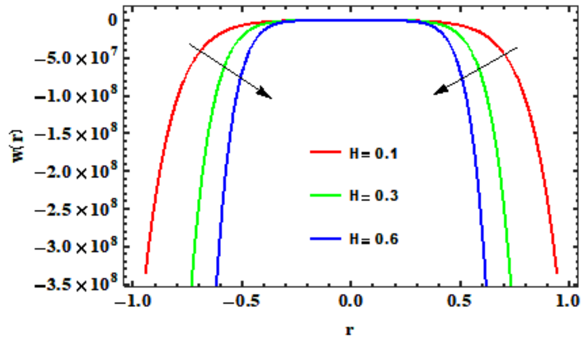

Figure 2-Velocity variation vs. H at $m = 10, \lambda = 1, b = 0.1, D_e = 1, \gamma = 0.1$

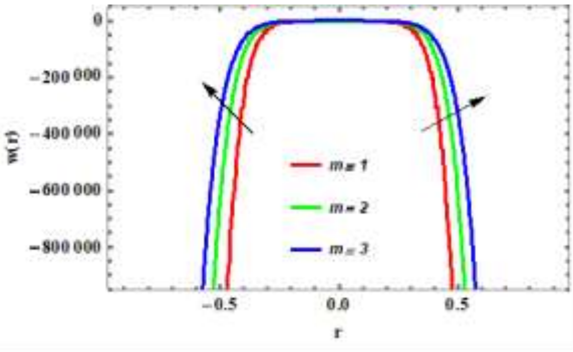

Figure 3-Velocity variation vs. m at $H = 0.3, \lambda = 1, b = 0.1, D_e = 1, \gamma = 0.1$

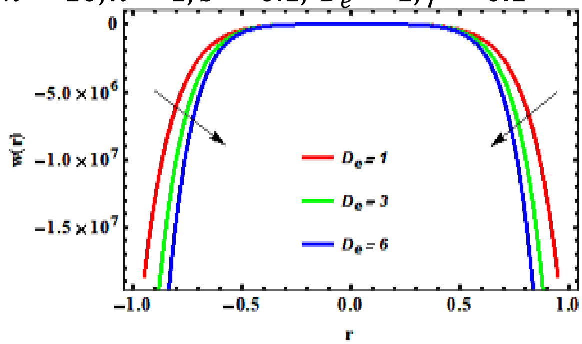

Figure 4-Velocity variation vs. D_e at $H = 0.3, m = 10, \lambda = 1, b = 0.1, \gamma = 0.1$

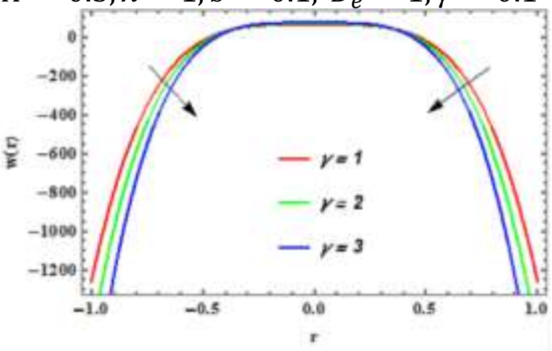

Figure 5-Velocity variation vs. γ at $H = 0.3, m = 10, \lambda = 1, b = 0.1, D_e = 1$

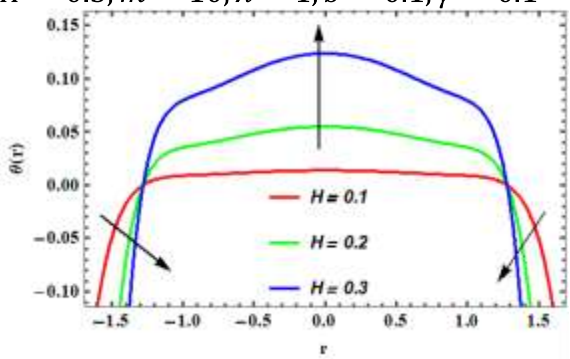

Figure 6-Temperature variation vs.H at , $m = 10, B_r = 0.5, D_u = 0.3, \beta_t = 0.6$

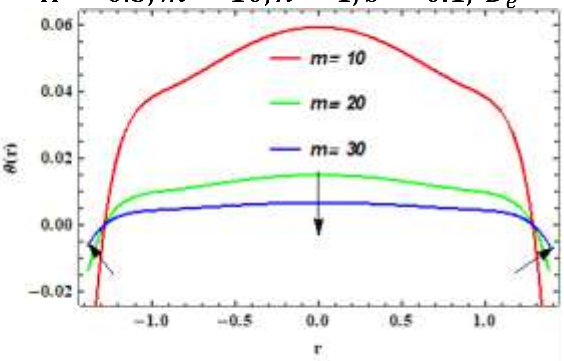

Figure 7-Temperature variation vs. m at $H = 0.1, \beta_t = 0.6, B_r = 0.5, D_u = 0.3$

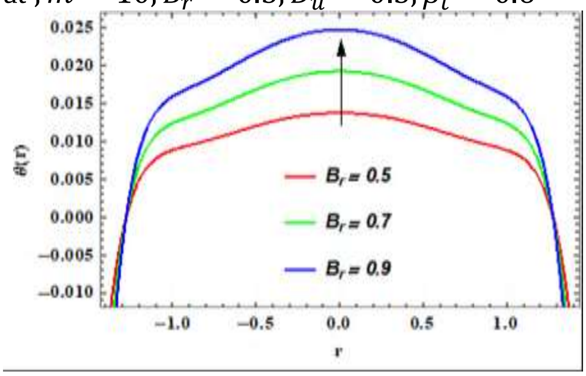

Figure 8-Temperature variation vs.B_r at $H = 0.1, m = 10, \beta_t = 0.6, D_u = 0.3$

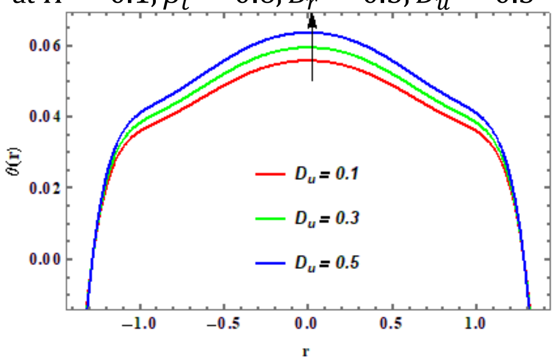

Figure 9-Temperature variation vs. D_u at $H = 0.1, m = 10, B_r = 0.5, \beta_t = 0.6$

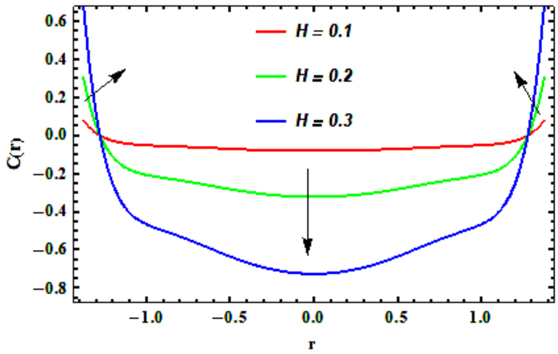

Figure 10-Concentration variation vs.H at $S_c = 0.1, m = 0.2, \beta_c = 0.6, S_r = 0.6$

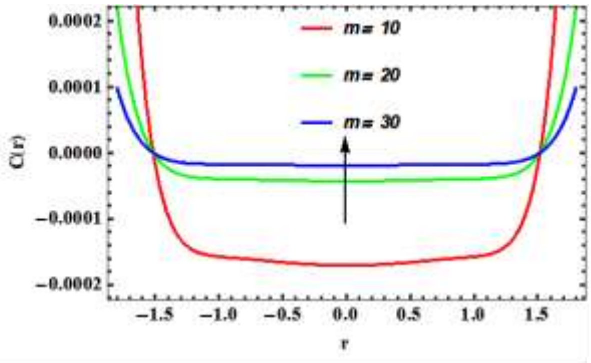

Figure 11-Concentration variation vs. m at $H = 0.1, S_c = 0.1, \beta_c = 0.6, S_r = 0.6$

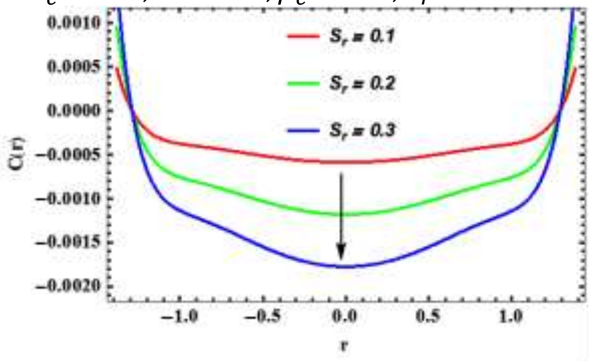

Figure 12-Concentration variation vs. S_r at $S_c = 0.1, m = 0.2, \beta_c = 0.6, H = 0.1$

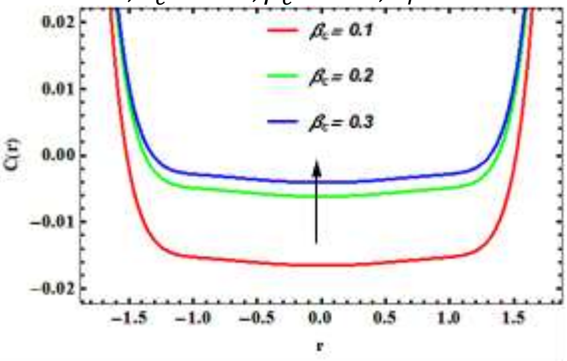

Figure 13-Concentration variation vs.β_c at $H = 0.1, S_c = 0.1, m = 0.2, S_r = 0.6$

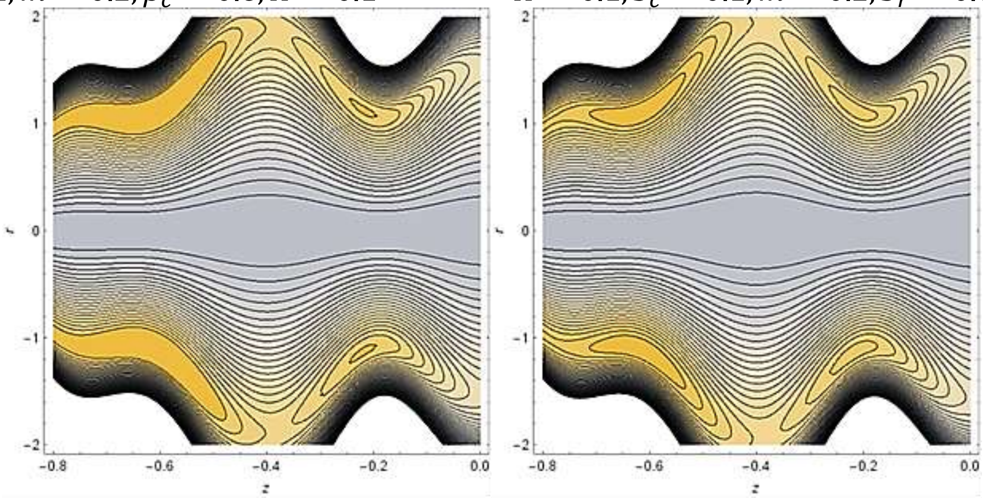

Figure 14-Stream function variation vs.r H at , $m = 10, b = 0.1,\ D_e = 1, \gamma = 0.1$

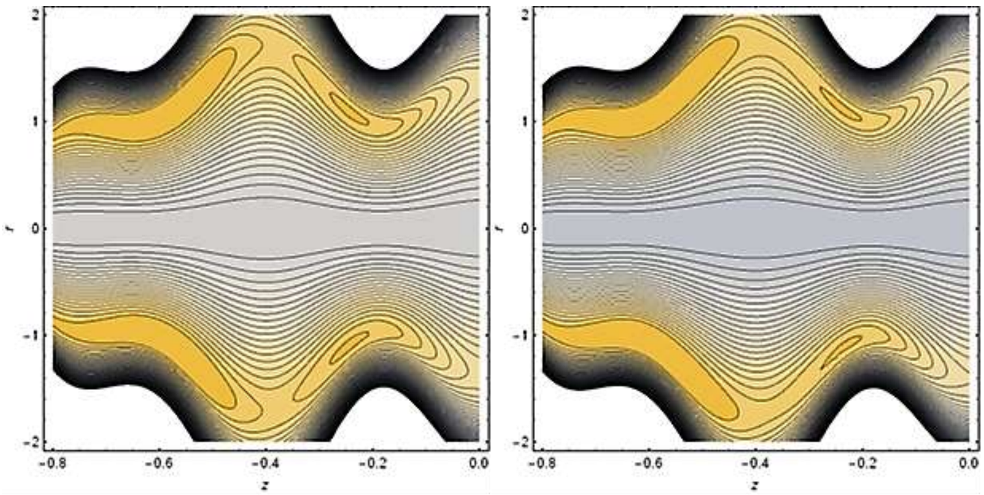

Figure 15-Stream function variation vs. D_e at , $H = 0.1, b = 0.1, m = 10, \gamma = 0.1$

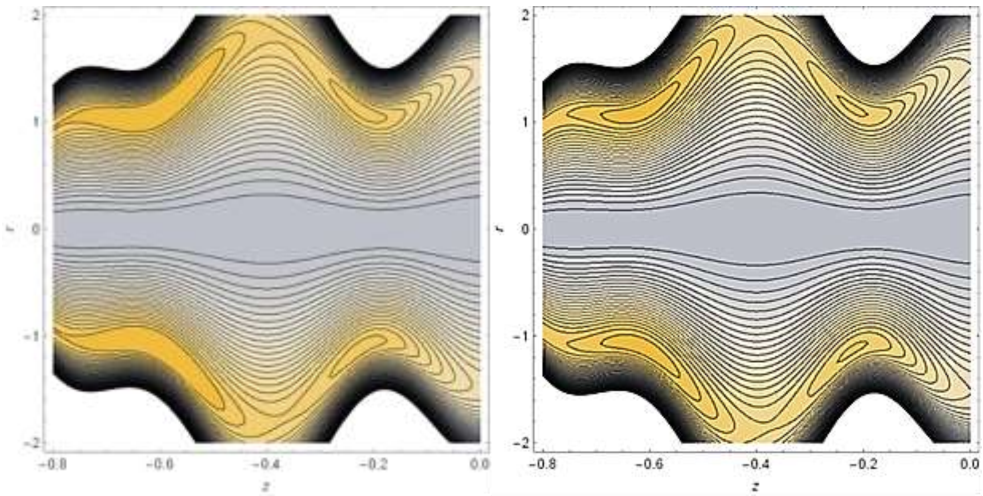

Figure 16-Stream function variation vs. γ at $m = 10, b = 0.1,\ D_e = 1, H = 0.1$

5. Conclusions

In this article, we have analyzed the role of the Hartman number, the Hall current, the Deborah number, the slip parameter, the Brickman number, the Dufour number, the Soret number, and the mass transfer Biot number on the peristaltic motion of a non-Newtonian Fene-P fluid flow in the tapered tube. Based on what was previously mentioned, it can be concluded that an increase in the Hartman number H, the Deborah number D_e, and the slip parameter γ show a deceleration in the velocity of the fluid while the velocity exhibits an accelerated attitude as the Hall current m increases. The Hartman number H and the Hall current m show opposite behavior for temperature distribution and mass diffusion, and we show that the temperature profile rises as the Brickman number B_r and the Dufour number $D_u$increase. An increase in the values of the Soret number S_r leads to a reduction in mass diffusion. Whereas a boost in the mass transfer Biot number β_c leads to a rise in concentration. The Hartman number H and the slip parameter γ cause a reduction in the size of the trapping bolus, but the number of trapping bolus increases.

References

[1] S. K. Rabiha and M. A. Ahmed, "Effect of MHD and Porous Media on Nanofluid Flow with Heat Transfer: Numerical Treatment," Journal of Advance Research in Fluid Mechanics and Thermal Sciences, vol. 63, no. 2, pp. 317-328, 2019.

[2] S. H. Saba and M. A. Ahmed, "Analytical Study of Soret and Dufour effect in the Electro-osmotic peristaltic flow of Rabinowitsch fluid model," Ibn AL-Haitham Journal For Pure and Applied Sciences, vol. 34, no. 2, pp. 70-86, 2021.

[3] S. H. Saba and M. A. Ahmed, "Influence of a Rotating Frame on the Peristaltic Flow of a Rabinowitsch Fluid Model in an Inclined Channel," Journal of Al-Qadisiyah for Computer Science and Mathematics, vol. 12, no. 1, pp. 21-33, 2020.

[4] S. H. Saba and M. A. Ahmed, "MHD Effect on Peristaltic Transport for Rabinowitsch Fluid through A Porous Medium in Cilia Channel," Iraqi Journal of Science, vol. 61, no. 6, p. 1461–1472, 2020.

[5] M. Imran, A. Shaheen, E.-S. M. Sherif, M. Rahimi-Gorji and A. H. Seikh, "Analysis of peristaltic flow of Jeffrey six constant nano fluid in a," Chinese Journal of Physics, vol. 66, pp. 60-73, 2020.

[6] I. Naveed, J. Maryiam, S. Muhammad, S. Farooq and Q. Mubashir, "Outcome of slip features on the peristaltic flow of a Rabinowitsch nanofluid in an asymmetric flexible channel," Multidiscipline Modeling in Materials and Structures, vol. 17, no. 1, 2020.

[7] R. S. Mohammed and A. A. Hayat, "Approximate Treatment for The MHD Peristaltic Transport of Jeffrey Fluid in Inclined Tapered Asymmetric Channel with Effects of Heat Transfer and Porous Medium," Iraqi Journal of Science, vol. 61, no. 12, p. 3342–3354, 2020.

[8] S. K. Rabiha and M. A. Ahmed, "A study of MHD and Darcy-Forchheimer effects on third grade flow with Cattaneo-Christov heat flux," AIP Conference Proceedings 2292, 020001, 2020.

[9] N. Ali, S. Hussain and K. Ullah, "Theoretical analysis of two-layered electroosmotic peristaltic flow of FENE-P fluid in an axisymmetric tube," Phys. Fluids 32, 023105, 2020.

[10] Z. Asghar and N.Ali, "Analysis of Mixed Convective Heat and Mass Transfer on Peristaltic Flow of Fene-P Fluid with Chemical Reaction," Journal of Mechanics, vol. 32, no. 01, pp. 83-92, 2016.

[11] P. Oliveira, "Re duce d-stress method for efficient computation of time-dependent viscoelastic flow with stress equations of FENE-P type," Journal of Non-Newtonian Fluid Mechanics, vol. 248, pp. 74-91, 2017.

[12] M. Michael, R. Pedro, C. Thibaut, W. Mark, A. Alexandre, H. David and d. B. Gregory, "A FENE-P k− ε Viscoelastic Turbulence Model Valid up to High Drag Reduction without Friction Velocity Dependence," Appl. Sci., vol. 10, no. 8140, 2020.

[13] L. Khezzar, A. Filali and M. AlShehhi, "Flow and heat transfer of FENE-P fluids in ducts of various shapes:Effect of Newtonian solvent contribution," Journal of Non-Newtonian Fluid Mechanics, vol. 207, pp. 7-20, 2014.

[14] P. J. Oliveira, Covilhg and Portugal, "An exact solution for tube and slit flow of a FENE-P fluid," Springer,Acta Mechanica, vol. 158, pp. 157 -167, 2002.

[15] T. Hayat, A. Naseema, M. Rafiq and E. A. Fuad, "Hall and Joule heating effects on peristaltic flow of Powell–Eyring liquid in an inclined symmetric channel," Results in Physics, vol. 7, p. 518–528, 2017.

[16] T. E.-D. NABIL and R. M. DOAA, "Hall Current and Joule Heating Effects on Peristaltic Flow of a Sisko Fluid with Mild Stenosis through a Porous Medium in a Tapered Artery with Slip and Convective Boundary Conditions," Sains Malaysiana, vol. 49, no. 5, pp. 1175-1190, 2020.

[17] A.-H. A. Hanaa, "The effects of Joule heating and variable thermal conductivity on peristaltic pumping of Jeffrey nanofluid in the presence of heat transfer," Heat Transfer, vol. 49, no. 3, pp. 1237-1255, 2020.

[18] T. M. E. Nabil, M. A.-S. Osama, A. S. A.-S. Adel, A. A. ElShekhipy and H. Nada, "Peristaltic Transport of Magnetohydrodynamic Carreau Nanofluid with Heat and Mass Transfer inside Asymmetric Channel," American Journal of Computational Mathematics, vol. 07, no. 01, p. 20, 2017.

[19] Y. H. Rasha and A. A. Hayat, "Hall and Joule's heating Influences on Peristaltic Transport of Bingham plastic Fluid with Variable Viscosity in an Inclined Tapered Asymmetric Channel," Ibn AL-Haitham Journal For Pure and Applied Sciences, vol. 34, no. 1, 2021.

[20]A. A. Hayat, "Radiative peristaltic transport of Ree-Eyring fluid through porous medium in asymmetric channel subjected to combined effect of inclined MHD and convective conditions," Journal of Physics: Conference Series, vol. 1879, 2021.
[21]S. K. Rabiha and M. A. Ahmed, "Influences of Heat Transfer in Peristaltic Transport of Two-Layer Model," Journal of Al-Qadisiyah for Computer Science and Mathematics, vol. 12, no. 2, p. 19–29, 2020.
[22]S. K. Rabiha and M. A. Ahmed, "Impacts of Heat and Mass Transfer on Magneto Hydrodynamic Peristaltic Flow Having Temperature-dependent Properties in an Inclined Channel Through Porous Media," Iraqi Journal of Science, vol. 61, no. 4, p. 854–869, 2020.
[23]S. H. Saba and M. A. Ahmed, "Heat and mass impacts on peripheral layers of different viscosity on peristaltic flow of Rabinowitsch fluids," AIP Conference Proceedings 2292, 020007, 2020.
[24]B. Aneela and X. Hang, "Entropy Generation Analysis of Peristaltic Flow and Heat Transfer of a Jeffery Nanofluid in a Horizontal Channel under Magnetic Environment," Hindawi,Mathematical Problems in Engineering, p. 13, 2019.
[25]J. K. Bilal, A. J. Ameer and H. R. Ahmed, "The Influence of Convection Heat Transfers for Vertical Mini-Tubes Using Solvent Carbon Dioxide and Porous Media at Supercritical Pressure," Engineering and Technology Journal, vol. 39, no. 9, pp. 1409-1419, 2021.
[26]A. A. Kayser, J. A.-D. Mustafa and A. H. Ali, "Experimental Study of Vibration on Pipe Conveying Fluid at Different End Conditions for Different Fluid Temperatures," Engineering and Technology Journal, vol. 37, no. 12A, pp. 512-515, 2019.
[27]H. N. Ali, Pertubation Methods, new york, 2008.